

An Analytical Approach to Connectivity in Regular Neuronal Networks

Luciano da Fontoura Costa and Marconi Soares Barbosa
*Institute of Physics of São Carlos. University of São Paulo,
São Carlos, SP, PO Box 369, 13560-970, phone +55 162 73 9858,
FAX +55 162 71 3616, Brazil, luciano@if.sc.usp.br*
(Dated: October 5, 2018)

This paper describes how realistic neuromorphic networks can have their connectivity fully characterized in analytical fashion. By assuming that all neurons have the same shape and are regularly distributed along the two-dimensional orthogonal lattice with parameter Δ , it is possible to obtain the exact number of connections and cycles of any length from the autoconvolution function as well as from the respective spectral density derived from the adjacency matrix. It is shown that neuronal shape plays an important role in defining the spatial distribution of synapses in neuronal networks. In addition, we observe that neuromorphic networks typically exhibit an interesting phenomenon where the pattern of connections is progressively shifted along the spatial domain for increasing connection lengths. This is a consequence of the fact that in neurons the axon reference point usually does not coincide with the cell centre of mass. Morphological measurements for characterization of the spatial distribution of connections, including the adjacency matrix spectral density and the lacunarity of the connections, are suggested and illustrated. We also show that Hopfield networks with connectivity defined by different neuronal morphologies, quantified by the proposed analytical approach, lead to distinct performance for associative recall, as measured by the overlap index. The potential of the proposed approach is illustrated with respect to digital images of real neuronal cells.

PACS numbers: 89.75.Fb, 87.18.Sn, 02.10.Ox, 89.75.Da, 89.75.Hc

I. INTRODUCTION

A particularly meaningful way to understand neurons is as cells optimized for *selective connections*, i.e. connecting between themselves in a specific manner so as to achieve proper circuitry and behavior. Indeed, the intricate shape of dendritic trees provide the means for connecting with specific targets while minimizing both the cell volume and the implied metabolism (e.g. [1, 2]). While great attention has been placed on the importance of synaptic strength over the emerging neuronal behavior, geometrical features such as the shape and spatial distribution of the involved neurons are closely related to the network connectivity. In addition, the topographical organization and connections pervading the mammals' cortex provide further indication that adjacencies and spatial relationships are fundamental for information processing by biological neuronal networks. The importance of neuronal geometry has been reflected by the growing number of related works (see, for instance, [3]). However, most of such approaches target the characterization of neuronal morphology in terms of indirect and incomplete measures such as area, perimeter and fractal dimension of the dendritic and axonal arborizations. Interesting experimental results regarding the connectivity of neuronal cells growth *in vitro* have been reported in [4, 5] and what is possibly the first direct computational approach to neuronal connectivity was only recently reported in [6], involving the experimental estimation of the critical percolation density as neuronal cells are progressively superposed onto a two-dimensional domain. At the same time, the recent advances in complex network formalism (e.g. [7, 8, 9, 10, 11]) provide a wealthy of concepts and tools for addressing connectivity. Initial

applications of such a theory to bridge the gap between neuronal shape and function were reported in [12, 13].

As the investigation of the relationship between neuronal shape and function is underlined by computational approaches involving numerical methods and simulation, a need arises to develop an analytical framework for neuromorphic characterization that could lead to additional insights and theoretical results regarding the relationship between neuronal shape and function. The present work describes an analytical approach capable of fully characterizing the connectivity of morphologically-realistic neuronal networks composed by repetitions of the same neuron along space. Such a kind of network can be considered as a model of biological neuronal systems characterized by planarity and morphologic regularity, as is the case with ganglion cell retinal mosaics [14] and the basal dendritic arborization of cortical pyramidal cells. The basic idea underlying the proposed analytical approach is to use the symmetries induced by the periodical boundary conditions in order to allow the connecting matrix describing the network to become a circulant matrix. Important features such as the number of connections and cycles can then be exactly obtained from the spectrum of this matrix. Lacunarity is also considered as a complementary measurement of the connectivity pattern. The effect of different neuronal shapes over the dynamics of the respective neuronal systems (Hopfield) built upon such connections is then investigated by using the proposed methodology. It is shown that neuronal shape not only plays an important role in defining the spatial distribution of synapses in neuronal networks, but also imposes critical constraints over the respective behavior.

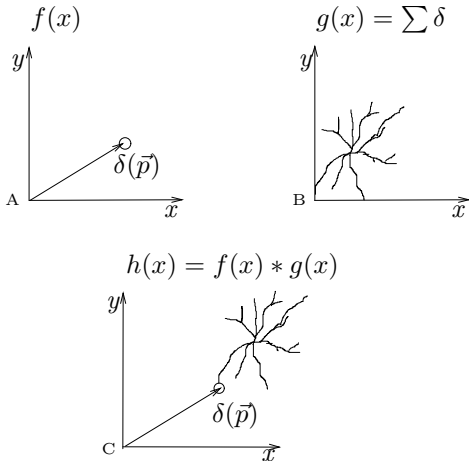


FIG. 1: The convolution of an axon function and a dendritic distribution

II. METHODOLOGY

The analytical representation of the connectivity of a neuronal network developed in the current section is based on the convolution of a function representing the neuronal cell with Dirac deltas. The basic adopted construction is illustrated in Figure 1, where the convolution of the neuronal cell $g(x)$ in (b) with the Dirac delta $f(x)$ in (a) produces as effect a copy of the original cell at the position of the delta (c). This can be mathematically expressed as:

$$\delta(\vec{a}) * g(\vec{x}) = g(\vec{x} - \vec{a}) \quad (1)$$

Let the neuronal cell be represented in terms of the triple $\eta = [A, S, D]$ where A is the set of points belonging to its axonal arborization, S is the set of points corresponding to the respective soma (neuronal body) and D are the dendritic arborization points. For simplicity's sake, a finite and discrete neuronal model is considered prior to its continuous general formulation. We therefore assume that the points used to represent the neuron belong to the square orthogonal lattice $\Omega = \{1, 2, \dots, N\} \times \{1, 2, \dots, N\}$, with parameter $\Delta = 1$. The axon and soma are represented by a single point each. Such points could be understood as corresponding to the tip of the axon and the soma center of mass, respectively. The dendritic arborization is represented in terms of the finite set of dendrite points $D = D_1, D_2, \dots, D_M$ and, in order to prevent the formation of loops, it is henceforth assumed that a dendrite point never coincides with the axon. Figure 2 illustrates such a geometrical representation for a neuron with 3 dendrite points. Observe that the coordinate origin coincides with the axon, which is taken as reference for the soma and dendrite coordinates. Observe that the arrows in this figure refer to the relative positions of the soma and dendrites and not to the signal

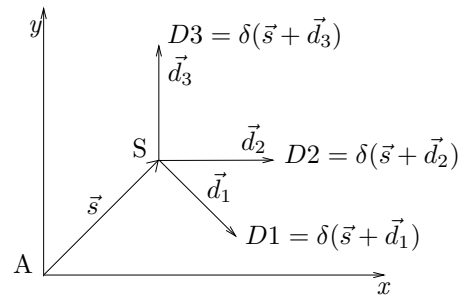


FIG. 2: The geometry of a simplified neuronal cells represented in terms of its axon A , soma centroid S and dendrite points D_i .

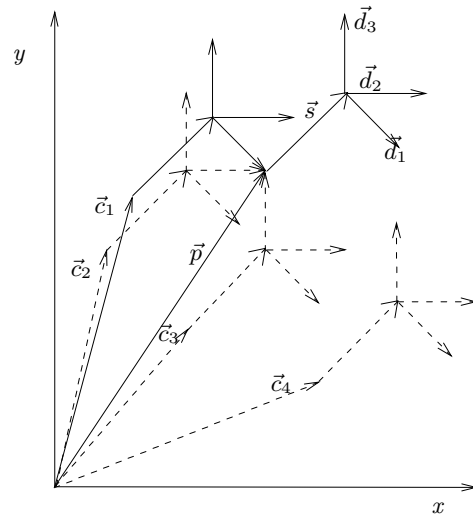


FIG. 3: The neurons connected through unit-length paths to neuron i which is placed with its axon A at \vec{p} can be obtained through the convolution between the position $\delta(\vec{p})$ of neuron i with the dendritic structure function.

transmission by a real neuronal cell, which occurs in the opposite direction (i.e. from dendrites to axon).

Neuromorphic networks (actually digraphs [8]) can now be obtained by placing one such a neuron at all possible nodes of the orthogonal lattice Ω .

A connection is established whenever an axon is overlaid onto a dendrite point. The thus obtained connection pattern stands out as a particularly important feature of the obtained network, as it defines the possible communications between the cells. Consequently, it is important to obtain analytical expressions describing the respective neuronal connectivity, e.g. by considering the spatial distribution of paths and cycles of any specific length along the network.

We start by considering the connections with a single specific neuron i placed with its axon at position \vec{p} , illustrated in Figure 3 together with four other neuronal cells at positions $\vec{c}_1, \vec{c}_2, \vec{c}_3$ and \vec{c}_4 . Given the particular geometry of the basic cell, three connections are implied with

the cells at \vec{c}_1 , \vec{c}_2 and \vec{c}_3 whose dendrites coincide with the axon of the cell i . In the case of cell \vec{c}_1 , this situation can be mathematically expressed as $\vec{c}_1 = \vec{p} - \vec{d}_1 - \vec{s}$. The fourth cell \vec{c}_4 illustrates one of the many neurons which are *not* connected to cell i . Two directly connected cells are henceforth represented as two nodes of a graph connected by a unit-length path (a simple arc).

As is clear from such a construction, the set of neurons connected to i through unit-length paths can be obtained by convolving the initial point [18] $\delta(\vec{p})$ (the tip of the axon) with the function $g(x, y)$ representing the neuronal cell

$$g(x, y) = \delta(-\vec{d}_1 - \vec{s}) + \delta(-\vec{d}_2 - \vec{s}) + \delta(-\vec{d}_3 - \vec{s}). \quad (2)$$

Observe that the minus signs in this equation are implied by the need to flip the function representing the cell shape along both axes, so as to obtain proper propagation of the connections. For instance, in Figure 3, the propagation of information proceeds from the original axon at \vec{p} to the dendrites at \vec{c}_1 , \vec{c}_2 , and \vec{c}_3 .

More generally given a set of initial neurons with axons represented as a Dirac's delta distribution $\xi(x, y)$, the density of dendrites connected to those neurons by unit-path lengths can be obtained from Equation 3. Observe that $\xi(x, y)$ may contain Dirac deltas with intensity larger than one, resulting from sums of coinciding deltas. The function $\nu(x, y)$ in Equation 4 is analogous to $\xi(x, y)$ but here all Dirac deltas have unit intensity. The functions expressing the density of the dendrites connected to the original neurons through paths of length k is given by Equation 5. The number of connections with length k is given by Equation 6. Observe that the use of the Dirac delta function in such a formulation allows the immediate extension of such results to continuous spatial domains.

While the analytical characterization of the connectivity of the considered network model has been allowed by the fact that identical neuronal shapes are distributed along all points of the orthogonal lattice, it is interesting to consider extensions of such an approach to other situations. An immediate possibility is to consider sparser configurations, characterized by larger lattice parameters Δ . Such an extension involves sampling the neuronal cell image at larger steps.

$$\chi(x, y) = g(x, y) * \xi(x, y) \quad (3)$$

$$\nu(x, y) = \begin{cases} \delta(x, y) & \text{if } \xi(x, y) \neq 0 \\ 0 & \text{otherwise.} \end{cases} \quad (4)$$

$$\chi_k(x, y) = \underbrace{g(x, y) * \dots * g(x, y)}_{k \times} \xi(x, y) \quad (5)$$

$$\tau_k(x, y) = \sum_{j=1}^k (\chi_j(x, y)) \quad (6)$$

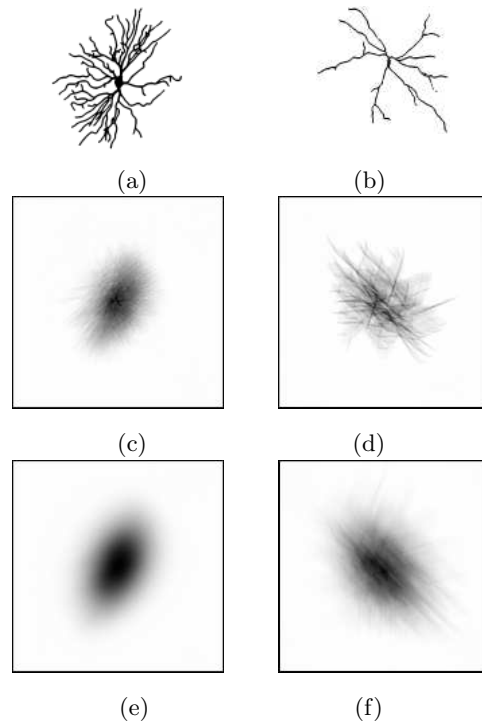


FIG. 4: Two real neuronal cells (a-b) and their respective total number of connections of length $k = 2$ (c-d) and 3 (e-f). The axon has been placed at the cell centroid (considering soma plus dendrites). The neuronal cell figures in (a) and (b) are adapted with permission from [14].

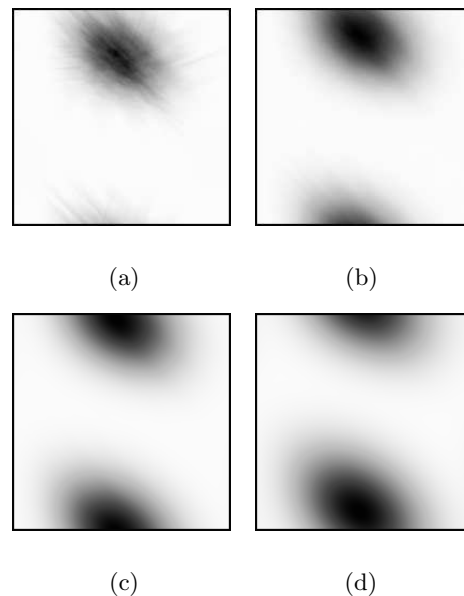


FIG. 5: The total number of connections of length $k = 1$ (a), 2 (b), 3 (c) and 4 (d) for the neuronal cell in Figure 4(a) with the axon placed over the cell centroid, which is itself displaced from the cell centroid by $\vec{s} = (0, 7)$ pixels.

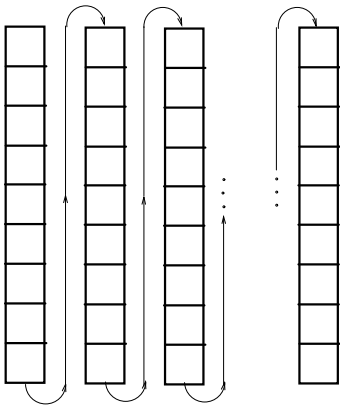


FIG. 6: The circulating scheme.

Figure 4 shows two digital images obtained from real ganglion cells, (a) and (b), and their respective functions $\chi_k(x, y)$ for $k = 2$ and 3. The axon has been placed over the centroid of the neuronal shape (including soma and dendrites), whereas the dendritic trees have been spatially sampled into 2033 and 671 pixels, respectively. Figure 5 shows $\chi_k(x, y)$ obtained for the cell in Figure 4(a) but with the soma located at the cell center of mass, which is displaced from the cell centroid by $\vec{s} = (0, 7)$ pixels. It is clear from such results that the neuron morphology strongly determines the connectivity between cells in two important senses: (i) the spatial scattering of the dendrite points influences the connectivity distribution and (ii) the relative position of the axon defines how the centroid of the connections shifts for increasing values of k . While the increased number of synaptic connections implied by denser neuronal shapes is as expected, it is clear from the example in Figure 5 that the distance from axon to cell center of mass implies spatial displacement of the connection pattern. Given the predominantly two-dimensional structure of the mammals' cortex, such an effect provides an interesting means to transmit information horizontally along such structures. In other words, faster signal transmission along the cortical surface is achieved whenever the axon is placed further away from the dendritic tree. As the proper characterization, classification, analysis and simulation of neuromorphic networks are all affected by these two interesting phenomena, it is important to derive objective related measurements. The next section addresses the characterization of the morphology of such networks.

III. MORPHOLOGY

Let $P(x, y)$ be a density function obtained by normalizing $\chi_k(x, y)$, i.e.

$$P(x, y) = \frac{\chi(x, y)}{\int_{-\infty}^{\infty} \chi(x, y) dx dy} \quad (7)$$

Thus, the spatial scattering of the connections can be quantified in terms of the respective covariance matrix K_k , and the spatial displacement of the centroid of $P(x, y)$ can be quantified in terms of the 'speed' $v = \|\vec{s}\|$. Additional geometrical measurements of the evolution of the neuronal connectivity that can be derived from the covariance matrix K include the angle α_k that the distribution main axis makes with the x-axis and the ratio ρ_k between the largest and smallest respective eigenvalues.

Another interesting network feature related to connectivity is its number $C_{\ell, k}$ of cycles of length ℓ established by the synaptic connections. This feature can be calculated from the enlarged matrix A obtained by stacking the columns of the matrix where the neuronal cell image is represented in order to obtain the rows of A , while the reference point of the cell is shifted along the main diagonal of A . Figure 6 presents the boundary conditions adopted for the orthogonal lattice Ω underlying the neuronal structure. The first line of matrix A corresponds to the whole structure in this figure, starting from the upper left-most cell and following the arrows. The second line of A is obtained similarly, but the structure is mounted circularly from the element (2,2) of A , and so on. As a consequence of such assumptions, A becomes a circulant matrix. Observe that studies involving non-periodical boundary conditions can be approximated by using large image sizes $N \times N$.

The N^2 eigenvalues of the thus obtained *adjacency matrix* [7] of the whole two-dimensional network are henceforth represented as λ_i , $i = 1, 2, \dots, N^2$. As A is circulant, these eigenvalues can be immediately obtained from the Fourier transform of its first row. Observe that the simplicity and speed of such an approach allow for systematic investigation of a variety of different neuronal shapes. As the cell reference point is assumed never to coincide with a dendrite point, we also have that $\sum_{r=1}^N \lambda_r = 0$. As A is a non-negative matrix, there will always be a non-negative eigenvalue λ_M , called the *dominant eigenvalue of A* , such that $\lambda_r \leq \lambda_M$ for any $r = 1, 2, \dots, N$. The *spectral density* (e.g. [7]) of the adjacency matrix, defined in Equation 8, where λ_p is the p -th eigenvalue of A , provides an additional way to characterize the topology of the obtained networks.

$$\rho(\lambda) = \frac{1}{N} \sum_{r=1}^N \delta(\lambda - \lambda_r) \quad (8)$$

The eigenvalue λ_M , which depends on the specific dynamics through which new edges are incorporated into

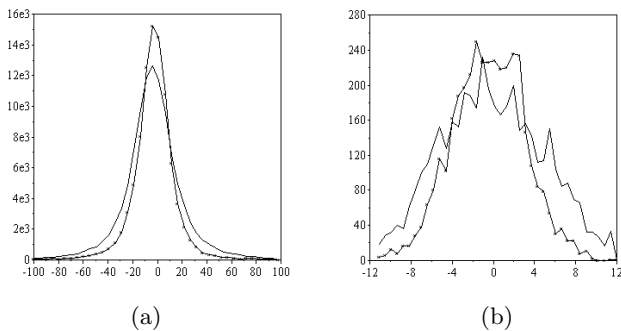


FIG. 7: Spectral density of the adjacency matrices obtained for the neuronal cells in Figure 4 considering $\Delta = 1$ (a) and $\Delta = 5$ (b). The crossed lines refer to the sparser neuronal cell.

the network, represents an interesting parameter for characterizing the cyclic composition of complex networks. Figures 7(a) and (b) show the real part (recall that the adjacency matrix for a digraph is not necessarily symmetric) of the spectral density of the adjacency matrices obtained for the neuronal cells in Figure 4(a) and (b) considering lattice spacings $\Delta = 1$ and 5. The wider dispersion of the spectrum of the denser cell in Figure 7(a) reflects a higher potential for connections of that neuron in both cases. It is also clear that the separation of cells by $\Delta = 5$ leads to a substantially smaller spectrum, with immediate implications for the respective neuronal connectivity.

An additional morphological property of the spatial distribution of the connections is their respective *lacunarity* (e.g. [16]), which expresses the degree of translational invariance of the obtained densities. Figure 8 shows the lacunarities of the connection densities obtained for the two considered cells with respect to $k = 1$ to 4. It is interesting to observe that most of the lacunarity differences are observed for $k = 1$, with similar curves being obtained for larger values of k . At the same time, the denser cell led to lower lacunarity values. Given their immediate implications for neuronal connectivity, the above proposed set of neuronal shape measurements present specially good potential for neuron characterization and classification.

IV. ASSOCIATIVE RECALL

One of the most important functional properties of Hopfield neuronal networks is their associative recall, which can be quantified by the overlap measurement, obtained by comparing the originally trained and the recovered patterns. A Hopfield network is completely determined by its respective connecting matrix, which in the case of the models considered in the present work is constrained by the adjacency matrix derived from the morphological structure in the sense that only the

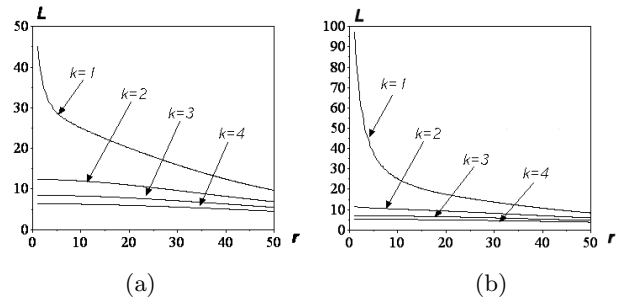


FIG. 8: Lacunarity for the spatial distributions of connections for the cells in Figure 4.

weights corresponding to existing connections are allowed to vary [13]. Therefore, the shape of the neuron has a direct impact on the performance of the network, which is chiefly dictated by the null-space of the adjacency matrix spectrum [17]. The analytical approach introduced in the current work can be immediately used for the estimation of overlaps considering different neuronal shapes.

In the standard Hopfield setup the cells are either firing ($S_i = 1$) or silent ($S_i = -1$) and are updated according to the rule

$$S_i \rightarrow \text{sign}\left(\sum_k J_{ik} S_k\right) \quad (9)$$

with synaptic strengths $J_{ik} = \sum_{\mu} \xi_i^{\mu} \xi_k^{\mu}$ (Hebb rule) if i and k are connected, where $\xi_i^{\mu} = \pm 1$, $\mu = 1, 2, \dots, P$, are P random bit-strings called input patterns, and one of them, perturbed uniformly along its extent, is supposed to be recalled by this updating rule (i.e. associative memory). The quality of recall is measured by the overlap $\Psi = \sum_i S_i \xi_i^1$ if the first pattern is supposed to be recovered.

We consider the simple prototypical cell patterns presented in Figure 9. A network was obtained for each cell shape by using the above formalism, and a non-randomly diluted Hopfield model with such connection matrix was then implemented for the networks and serially repeated a hundred times to gain statistical significance. All three networks consist of 441 neurons and the memory model is set to recall 25 background patterns with 20 percent of noise. For efficiency's sake, the recovering stage stops whenever a stable point (or reasonable fixed limit) is reached. To incorporate the effect of changing the axons position, which is potentially significant from the biological point of view, we disturbed the reference point of the axon randomly and gradually. This allowed us to study the robustness of the memory model.

Figure 10 shows the overlaps obtained while considering three simple neuronal shapes, namely the artificial neuronal cell shown in Figure 9, a line and a cross. For each cell pattern we have three overlap curves representing respectively: the lattice as it is, a perturbed version with one percent of uniform noise (in pixels), and

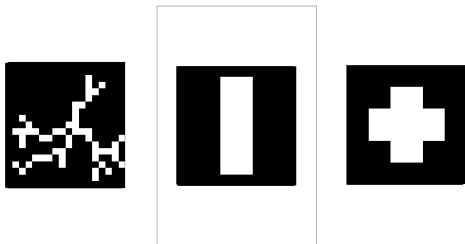


FIG. 9: Three prototypical cell shapes used in the morphological Hopfield simulation.

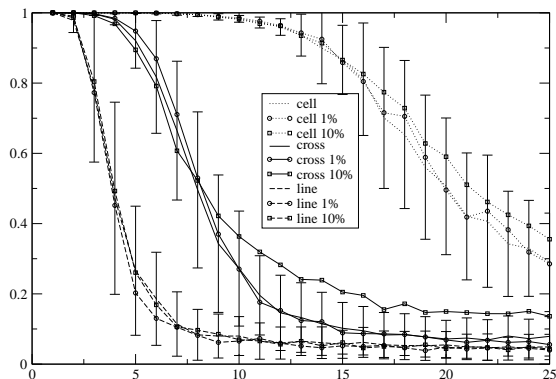


FIG. 10: The overlap curves for three different cell shapes shown in Figure 9.

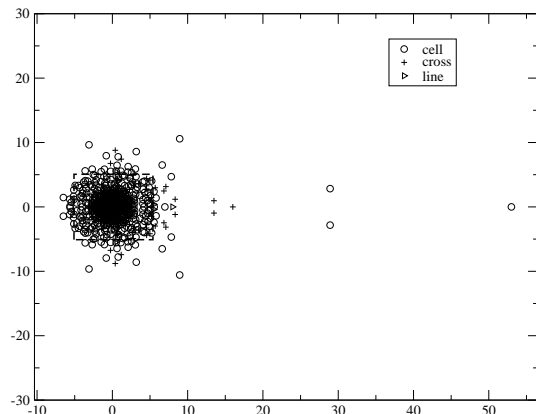


FIG. 11: The spectrum of the A matrix (represented in the complex plane) for the three different cell shapes shown in Figure 9, the marked inset is zoomed in Figure 12.

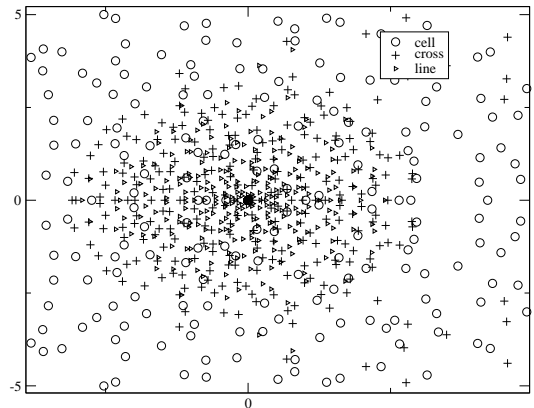


FIG. 12: The spectrum of the A matrix zoomed from the inset of Figure 11, showing the spread in the distribution of eigenvalues for the considered patterns.

another perturbed version with ten percent noise. Although the influence of such perturbations are masked by the stochastic nature of the system, we can see that as far the overlaps are taken as an indication of performance, the model is robust to network topology changes and sensitive to neuronal shape. An order clearly emerged in the overlaps albeit, as indicated by the large deviation, it is a visibly degenerated morphological measure. The more spatially distributed shapes tended to lead to better performance. The eigenvalues for each of the three considered cases are illustrated graphically in Figure 11. It is clear from this figure that the eigenvalues tend to organize symmetrically with respect to the real axis. Also, the eigenvalue dispersions obtained for the cases line, cross and cell tended to be progressively broader, reflecting their original spatial structure. In other words, shapes more uniform and isotropically distributed along space tended to produce broader eigenvalue distributions. The better overlap figures obtained for sparser patterns is closely related to the fact that more distributed eigenvalues are obtained in those cases, reducing the null space for memory representation.

V. CONCLUSIONS

An analytical approach to the characterization of neuronal connectivity was proposed and illustrated with respect to synthetic and real neurons. It was shown that the connections of progressive length established along the neuronal structure can be precisely quantified in terms of the autoconvolution of the function representing the individual shape of the neuron. The analysis of the connectivity pattern in terms of spectral dispersion and

lacunarity was also proposed and illustrated. In addition, we have shown that, by assuming a specific type of periodical boundary condition, it is possible to construct a circulant matrix whose spectrum can be conveniently calculated and used to characterize the topological and functional properties of the neuronal structure. More specifically, we implemented Hopfield networks having weight matrices constrained by the adjacency matrices defined by the individual neuronal cell geometry. The performance of such networks, quantified in terms of the overlap measurement, were shown to be strongly related to the morphology of the adopted neurons.

In addition to paving the way for the analytical characterization of the connections in regular neuromorphic networks, the framework proposed in this article can be immediately adapted to study the spread of waves of neuronal *activity* starting from the stimulus $\xi(x, y)$, where the neurons are understood to accept input and produce output in synchronous manner at each clock cycle T . For instance, the situation where the neuronal cells output corresponds to the inner product between its shape and

the respective area of the input space can be immediately characterized in terms of the eigenvalues and eigenvectors of precisely the same adjacency matrix A constructed as described above. Although the proposed methodology assumes identical, uniformly distributed neuronal cells, it is expected that they provide a reference model for investigating and characterizing real networks characterized by a certain degree of regularity, such as some subsystems found in the retina and cortex. Preliminary corroborations of such a possibility were provided by the fact that our overlap simulations tended to be robust to lattice perturbations. Mean-field extensions of the reported approach are currently being validated.

Acknowledgments

The authors are grateful to FAPESP (processes 99/12765-2, 96/05497-3 and 02/02504-01) and CNPq for financial support.

-
- [1] J. Karbowski, Phys. Rev. Lett. **86**, 3674 (2001).
 - [2] D. Purves and J. W. Lichtman, *Principles of Neural Development* (Sinauer, 1985).
 - [3] L. da F. Costa, Brain and Mind **4**, 1 (2003), special issue.
 - [4] O. Shefi, I. Golding, R. Segev, E. Ben-Jacob, and A. Ayali, Phys. Rev. E **66**, 021905 (2002).
 - [5] R. Segev, M. Benveniste, Y. Shapira, and E. Ben-Jacob, Phys. Rev. Lett. **90**, 168101 (2003).
 - [6] L. da F. Costa and E. T. M. Monteiro, Neuroinformatics **1**, 65 (2003).
 - [7] R. Albert and A. L. Barabási, Rev. Mod. Phys. **74**, 47 (2002).
 - [8] B. Bollobás, *Modern Graph Theory* (Springer-Verlag, New York, 2002).
 - [9] A. L. Barabási, E. Ravasz, and T. Vicsek, Physica A **259**, 559 (2001).
 - [10] F. Buckley and F. Harary, *Distance in Graphs* (Addison-Wesley, Redwood City, 1990).
 - [11] L. A. N. Amaral, A. Scala, M. Barthélémy, and H. E. Stanley, Proc. Natl. Acad. Sci. **97**, 11149 (2000).
 - [12] D. Stauffer, A. Aharony, L. da F. Costa, and J. Adler, Eur. J. Phys. (2003).
 - [13] L. da F. Costa, M. S. Barbosa, V. Coupez, and D. Stauffer, Brain and Mind **4**, 91 (2003).
 - [14] B. B. Boycott and H. Wässle, J. Physiol. **240**, 402 (1974).
 - [15] D. Stoyan, W. S. Kendall, and J. Mecke, *Stochastic Geometry and its Applications* (John Wiley and Sons, 1995).
 - [16] J. P. Hovi, A. Aharony, D. Stauffer, and B. B. Mandelbrot, Phys. Rev. Lett. **77**, 877 (1996).
 - [17] S. Haykin, *Neural Networks: A Comprehensive Foundation*, Prentice-Hall, Upper Saddle River, NJ, 2nd edition, 1999.
 - [18] Unless mentioned otherwise we will be using the simplifying notation for the dirac delta function $\delta(x-a) = \delta(a)$